DOI: 10.1002/ejic.200700317

Tetranuclear Nickel Complexes Composed of Pairs of Dinuclear LNi$_2$ Fragments Linked by 4,4′-Bipyrazolyl, 1,4-Bis(4′-pyrazolyl)benzene, and 4,4′-Bipyridazine: Synthesis, Structures, and Magnetic Properties

Vasile Lozan,[a] Pavlo Y. Solntsev,[b] Guido Leibeling,[c] Konstantin V. Domasevitch,*[b] and Berthold Kersting*[a]

Keywords: Macrocyclic ligands / Bipyrazolate ligands / Nickel / Polynuclear complexes / Magnetic properties

The ability of the ligands 4,4′-bipyrazolyl (H_2*bpz*), 1,4-bis(4′-pyrazolyl)benzene (H_2*bpzb*), and 4,4′-bipyridazine (*bpdz*) to link two dioctahedral LNi$_2$ units has been examined. The following complexes were prepared: $[L^1Ni^{II}_2(Hbpz)][BPh_4]$ (**6**$[BPh_4]$), $[L^1Ni^{II}_2(bpdz)][ClO_4]_2$ (**7**$[ClO_4]_2$), $[(L^1Ni^{II}_2)_2(bpzb)][BPh_4]_2$ (**8**$[BPh_4]_2$), and $[(L^2Ni^{II}_2)_2(bpz)][BPh_4]_2$ (**9**$[BPh_4]_2$), where $(L^1)^{2-}$ and $(L^2)^{2-}$ represent macrocyclic hexaaza-dithiophenolate ligands. All complexes have been characterised by UV/Vis spectroscopy, IR spectroscopy, and X-ray crystallography. Whereas $(Hbpz)^-$ and *bpdz* in **6**$[BPh_4]_2$ and **7**$[ClO_4]_2$ act as bidentate ligands coordinating to only one $[LNi_2]^{2+}$ unit, in **8**$[BPh_4]_2$ and **9**$[BPh_4]_2$ the $(bpzb)^{2-}$ and $(bpz)^{2-}$ units are tetradentate linkers. This is qualitatively explained in terms of the absence or presence of steric repulsions between the *t*Bu groups of the supporting ligands and the length of the coligands. The structures of the tetranuclear complexes differ mainly in the distance between the center of the Ni···Ni axes of the isostructural $[LNi_2]$ units {14.040(1) Å in **8**$[BPh_4]_2$, 9.184(1) Å in **9**$[BPh_4]_2$}. The two Ni$_2$-pyrazolato planes in **9**$[BPh_4]_2$ are coplanar. An analysis of the temperature-dependent magnetic susceptibility data for **9**$[BPh_4]_2$ reveals the presence of weak ferromagnetic exchange interactions between the Ni^{II} ions in the binuclear $[L^2Ni_2]$ subunits with values for the magnetic exchange constant J_1 of 23.97 cm^{-1} ($\mathbf{H} = -2JS_1S_2$). The exchange coupling across the dipyrazolato bridge is less than 0.1 cm^{-1}, suggesting that no significant interdimer exchange coupling occurs in **9**$[BPh_4]_2$.

Introduction

The coordination chemistry of the potentially quadridentate ligands 4,4′-bipyrazolyl (H_2*bpz*)[1,2] and its derivative 3,3′,5,5′-tetramethyl-4,4′-bipyrazolyl (H_2Me_4*bpz*)[3–6] has been studied in some detail, primarily due to their capability to form porous coordination polymers with potential uses as solid sorbents, ion exchangers or heterogeneous catalysts.[7–11] In this context, a large body of work has been carried out concerning the formation of polypyrazolate-based coordination networks with open framework structures.[12,13] It is surprising that such ligands have not yet been used in the construction of discrete polynuclear complexes. The oligonuclear Pd$_3$ and Pd$_4$ complexes reported by Yu et al. may serve as rather rare examples of this class of compounds.[14]

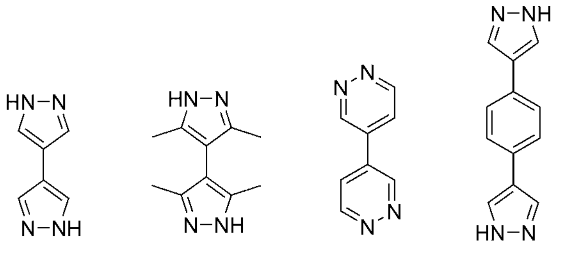

H_2*bpz* H_2Me_4*bpz* *bpdz* H_2*bpzb*

In previous work, we described a series of dinuclear transition-metal complexes of the macrocyclic N$_6$S$_2$ ligands L^1 and L^2 (Scheme 1).[15,16] These complexes have a rich coordination chemistry since the $[L^1M_2]^{2+}$ fragments are able to coordinate a large variety of coligands such as Cl^-,[15] OH^-,[17] NO_2^-, NO_3^-, N_3^-,[18] BH_4^-,[19] ClO_4^-, ReO_4^-, SO_4^{2-}, MoO_4^{2-},[20] $MoO_3(OMe)^-$,[21] and various carboxylate anions.[16,22,23]

The magnetic properties of an isostructural series of bioctahedral $[L^1M^{II}_2(OAc)]^+$ complexes have also been reported.[24] In the Mn$^{II}_2$, Fe$^{II}_2$ and Co$^{II}_2$ complexes of this

---

[a] Institut für Anorganische Chemie, Universität Leipzig,
Johannisallee 29, 04103 Leipzig
Fax: +49-341-973-6199
E-mail: b.kersting@uni-leipzig.de
[b] Inorganic Chemistry Department, Kiev University,
Volodimirska Street 64, Kiev 01033, Ukraine
E-mail: dk@anorgchemie.univ.kiev.ua
[c] Institut für Anorganische Chemie, Georg-August-Universität Göttingen,
37077 Göttingen, Germany

Supporting information for this article is available on the WWW under http://www.eurjic.org or from the author.

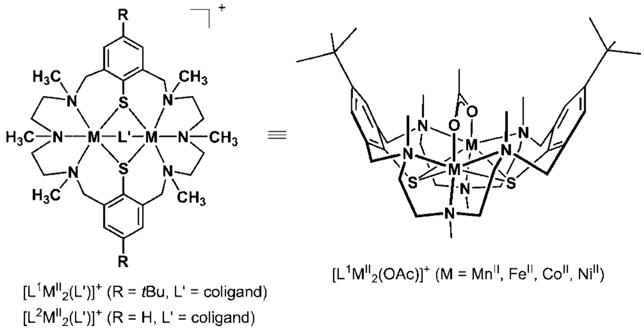

Scheme 1. Dinuclear complexes of the hexaaza-dithiophenolate ligands $(L^1)^{2-}$ and $(L^2)^{2-}$.

series intramolecular antiferromagnetic exchange interactions are present with J values of –5.1, –10.6, and –2.0 cm^{-1} ($\mathbf{H} = -2J\mathbf{S}_1\mathbf{S}_2$). For the corresponding Ni^{II}_2 complex, however, a ferromagnetic exchange interaction is observed (J = +6.4 cm^{-1}). In view of the strong interest in the targeted design of molecular-based magnetic materials using high-spin molecules of higher nuclearity,[25–31] we have initiated a study on the synthesis of complexes in which pairs of exchange coupled $[L^1Ni_2]$ units are linked by 4,4′-bipyrazole (H_2*bpz*) and 1,4-bis(4-pyrazolyl)-benzene (H_2*bpzb*). The neutral ligand 4,4′-bipyridazine (*bpdz*) was also included in this study. We report herein the results of our investigation together with the single-crystal X-ray structure determination of the complexes $[L^1Ni^{II}_2(H$*bpz*$)][BPh_4]$ (**6**$[BPh_4]$), $[L^1Ni^{II}_2($*bpdz*$)][ClO_4]_2$ (**7**$[ClO_4]_2$), $[(L^1Ni^{II}_2)_2($*bpzb*$)][BPh_4]_2$ (**8**$[BPh_4]_2$), and $[(L^2Ni^{II}_2)_2($*bpz*$)][BPh_4]_2$ (**9**$[BPh_4]_2$). The results of temperature-dependent magnetic susceptibility measurements on $[(L^2Ni^{II}_2)_2($*bpz*$)][BPh_4]_2$ (**9**$[BPh_4]_2$) are also described.

Results and Discussion

Synthesis of Ligands and Complexes

Of the N-heterocycles used in this study, only 4,4′-bipyrazolyl (H_2*bpz*) was reported previously.[1,2] Scheme 2 depicts the syntheses of the new compounds H_2*bpzb* and *bpdz*. The Diels–Alder reaction of bright-red 1,2,4,5-tetrazine (**1**) with *cis*-/*trans*-1,4-bis(dimethylamino)butadiene (**2**) in a 2.1:1 ratio is accompanied by a vigorous evolution of dinitrogen and affords after thermal elimination of dimethylamine and recrystallization from methanol colourless 4,4′-bipyridazine (*bpdz*) in reasonable yields (39%). The route to H_2*bpzb* began with a Vilsmeyer–Haack-type reaction of *p*-phenylenediacetic acid **3** with $POCl_3$/DMF to give the bis(trimethinium) salt **4**, which was isolated as its perchlorate salt.[32] Hydrolysis of **4** followed by treatment of the resulting tetraaldehyde **5** (not isolated) with hydrazine furnished the new dipyrazole derivative H_2*bpzb* as thin white needles in good overall yield (78%). The new compounds were of sufficient purity for metal complex syntheses.

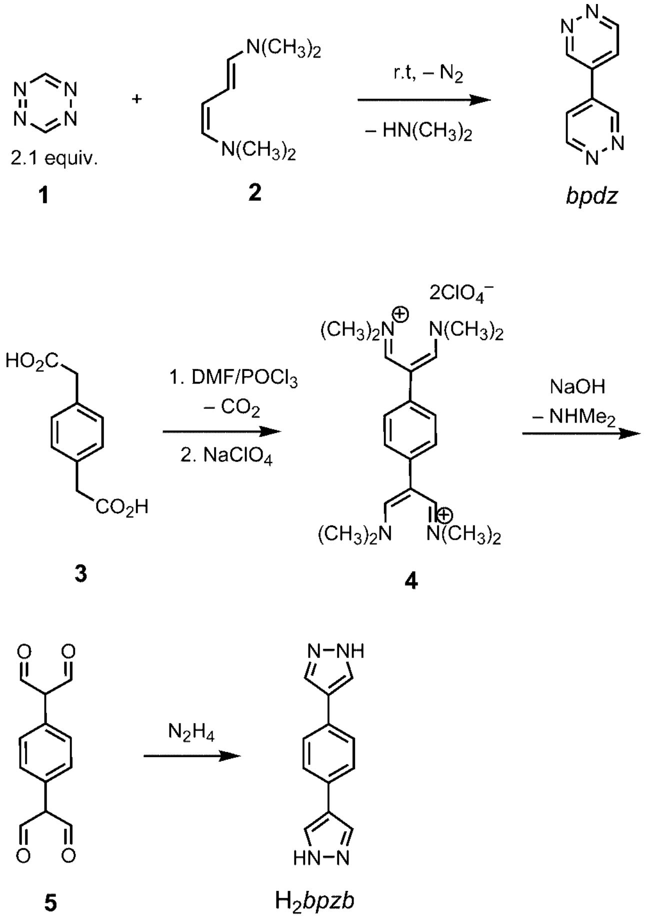

Scheme 2. Synthesis of the heterocycles H_2*bpzb* and *bpdz*.

Attempts to link two $[L^1Ni_2]^{2+}$ units by a $($*bpz*$)^{2-}$ dianion did not meet with any success. Treatment of $[L^1Ni_2Cl][ClO_4]$ with triethylammonium 4,4-bipyrazolate in methanol in varying molar ratios resulted always in the formation of the green 1:1 complex $[(L^1)Ni_2(H$*bpz*$)][ClO_4]$ (**6**$[ClO_4]$), presumably as a result of the sterically demanding *tert*-butyl groups. Nickel complexes of the neutral *bpdz* ligand were found to be inaccessible from $[L^1Ni_2Cl][ClO_4]$. The substitution reaction succeeded only with the more labile perchlorato complex $[L^1Ni_2(ClO_4)][ClO_4]$, but again only 1:1 complexes formed. Thus, treatment of a dark green acetonitrile solution of $[L^1Ni_2(ClO_4)][ClO_4]$ with *bpdz* produced a brown-yellow solution, from which brown crystals of $[L^1Ni_2(bpdz)][ClO_4]_2$ (**7**$[ClO_4]_2$) could be isolated in 80% yield.

It was clear at this stage that tetranuclear Ni_4 complexes would only be accessible with longer bipyrazolyls or with less bulky LNi_2 precursor subunits. Indeed, reaction of $[L^1Ni_2Cl][ClO_4]$ with a 0.5 molar equivalent of $($*bpzb*$)^{2-}$ (prepared in situ from H_2*bpzb* and NEt_3) in methanol followed by addition of an exess of $LiClO_4$ and recrystallization from acetonitrile affords the green complex $[(L^1Ni_2)_2($*bpzb*$)][ClO_4]_2$ (**8**$[ClO_4]_2$) in 76% yield. Similarly, reaction of $[L^2Ni_2Cl][ClO_4]$ with half a molar equivalent of $($*bpz*$)^{2-}$ in methanol followed by addition of an excess of $LiClO_4$ fur-

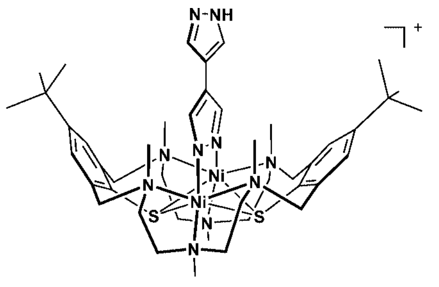

$[L^1Ni_2(Hbpz)]^+$ (**6**)

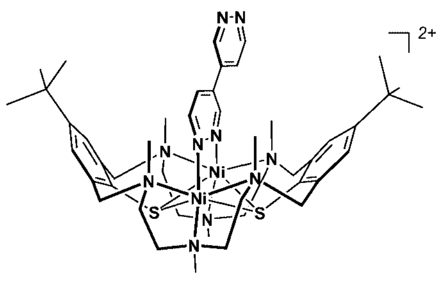

$[L^1Ni_2(bpdz)]^+$ (**7**)

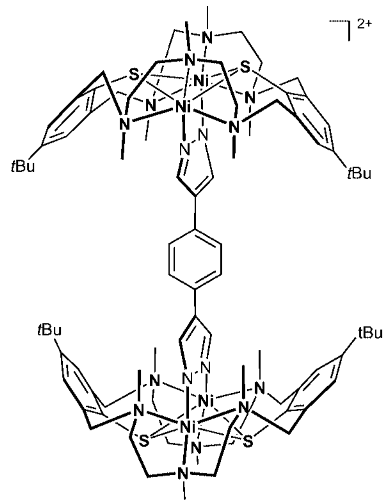

$[(L^1Ni)_2(bpzb)]^{2+}$ (**8**)

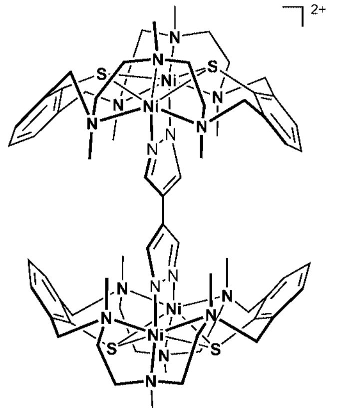

$[(L^2Ni)_2(bpz)]^{2+}$ (**9**)

nished the tetranuclear species $[(L^2Ni_2)_2(bpz)][ClO_4]_2$ (**9**$[ClO_4]_2$) as a dark-green, air-stable solid. Complexes **8** and **9** were also isolated as tetraphenylborate salts.

All compounds gave satisfactory elemental analyses and were characterized by IR spectroscopy and UV/Vis spectroscopy, and compounds **6**$[BPh_4]\cdot 1.5MeCN$, **7**$[ClO_4]_2\cdot 3MeCN$, **8**$[BPh_4]_2\cdot 6MeCN\cdot 2H_2O$, and **9**$[BPh_4]_2\cdot 2CH_2Cl_2$ also by X-ray structure analysis.

Characterization of the Complexes

Spectroscopic Characterization. IR and UV/Vis Spectroscopy

The infrared spectra of all compounds display the bands expected for the macrocyclic ligands and counterions, but were not informative with respect to the conformations of the supporting or coligands. Only the band at 3385 cm^{-1} in the IR spectrum of **6**$[BPh_4]$ can be attributed to the N–H stretching vibration of the protonated pyrazole moiety. The electronic absorption spectra of the nickel complexes have been recorded in the 300–1600 nm range in acetonitrile solution. The spectra of the pyrazolato complexes **6**, **8** and **9** display two weak absorption bands around 640 and 1190 nm typical of octahedral Ni^{II} ($S = 1$) ions. The observed values closely compare with those of $[L^1Ni_2(pz)]^+$ (*pz* = pyrazolate)[18] indicative of $\mu_{1,2}$-bridging pyrazolate functions and pseudo-octahedral N_4S_2 coordination environments around the Ni atoms. The UV/Vis spectrum of the bipyridazine complex **7**$[ClO_4]$ is similar but not identical with that of **6**$[BPh_4]$, displaying two weak bands at 608 and 1100 nm. The corresponding absorptions in previously reported $[L^1Ni_2(pydz)]^{2+}$ (*pydz* = pyridazine)[18] were observed at 615 and 1095 nm. The slight differences in the position of the d-d transitions indicate that each complex retains its integrity in solution.

X-ray Crystallography

Single-crystals of **6**$[BPh_4]\cdot 1.5MeCN$ were obtained by slow evaporation of a 1:1 acetonitrile/ethanol solution of **6**$[BPh_4]$. The crystal structure is composed of dinuclear $[L^1Ni_2(Hbpz)]^+$ cations, tetraphenylborate anions, and acetonitrile molecules of solvent of crystallization. An Ortep plot of the structure of complex **6** is depicted in Figure 1. Selected bond lengths and angles are summarized in Table 1. The bipyrazolato ligand acts only as a bidentate ligand towards one dinuclear $[L^1Ni^{II}_2]^{2+}$ unit through the ring atoms N(7) and N(8). The atoms N(9) and N(10) remain uncoordinated, but the hydrogen atom bonded to N(9) is involved in a hydrogen bonding interaction with an adjacent acetonitrile solvate molecule [N(9)···N(11)

2.975 Å]. The distance between the N atom of the acetonitrile and N(10) is 3.652 Å. The corresponding C–C, C–N, and N–N distances of the two five membered rings of the $(bpz)^{2-}$ dianion do not deviate significantly from each other; the largest difference being in the N–N bonds [N(7)–N(8) 1.384(2) Å, N(9)–N(10) 1.329(2) Å]. Note that the two heterocycles are not strictly coplanar. The dihedral angle between the two five-membered rings is 25.6°. The C(40)–C(42) bond is of length 1.472(2) Å indicative of a C–C single bond. The $[L^1Ni_2]^{2+}$ subunits in **6** and the compounds described below are structurally very similar, and the Ni–N and Ni–S distances lie within very narrow ranges (Table 1). The Ni···Ni distance is at 3.373(1) Å, which is nearly identical with that in $[L^1Ni_2(pz)][BPh_4]$ [3.389(1) Å].[18] Overall, this structure clearly shows that the bipyrazolate moiety cannot link two $[L^1Ni_2]^{2+}$ units. This can be attributed to the steric demand of the *t*Bu groups which hinder the formation of a tetranuclear complex. This assumption is nicely corroborated by the crystal structure determination of **9**$[BPh_4]_2$.

Figure 2 shows the structure of the dinuclear Ni^{II}_2 complex **7** in crystals of **7**$[ClO_4]_2$·3MeCN. Again, the 4,4′-bipyridazine ligand acts only as a bidentate group coordinating to only one bioctahedral $[L^1Ni_2]^{2+}$ entity through the ring nitrogen atoms N(7) and N(8). Metal complexes of 4,4′-bipyridazine have not been reported previously. The average Ni–$N_{pyridazine}$ bond length of 2.159(2) Å is significantly longer than the Ni–$N_{pyrazolate}$ distance in **6** [2.043(2) Å], implying that the neutral bipyridazine binds more weakly to the dinuclear $[L^1Ni_2]^{2+}$ fragment in **7** than

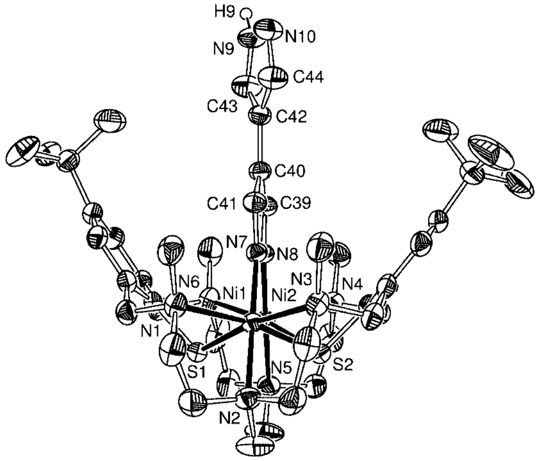

Figure 1. ORTEP representation of the structure of the $[L^1Ni^{II}_2(Hbpz)]^+$ cation in crystals of **6**$[BPh_4]$·1.5MeCN. Ellipsoids are represented at the 50% probability level. Hydrogen atoms except H(9) have been omitted for clarity.

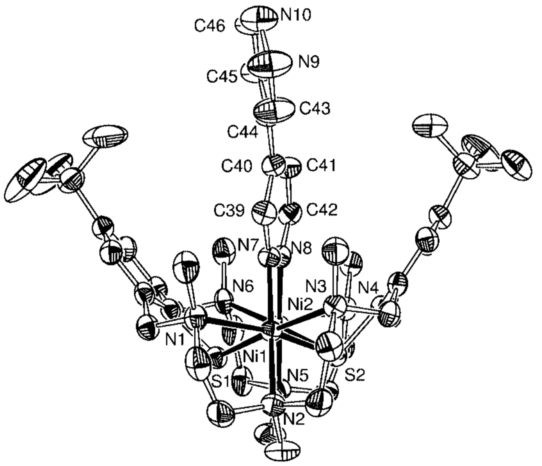

Figure 2. Structure of the $[L^1Ni^{II}_2(bpdz)]^{2+}$ dication in crystals of **7**$[ClO_4]_2$·3MeCN with thermal ellipsoids at the 50% probability level. Hydrogen atoms are omitted for reasons clarity.

Table 1. Selected bond lengths [Å] and angles [°] in **6**–**9**.

	6$[BPh_4]$·1.5MeCN	**7**$[ClO_4]_2$·3MeCN	**8**$[BPh_4]_2$·6MeCN·2H_2O	**9**$[BPh_4]_2$·2CH_2Cl_2
Ni(1)–N(7)	2.050(2)	2.149(3)	2.065(2)	2.037(2)
Ni(1)–N(1)	2.316(2)	2.352(3)	2.276(2)	2.430(2)
Ni(1)–N(2)	2.178(2)	2.125(3)	2.186(2)	2.170(2)
Ni(1)–N(3)	2.307(2)	2.255(3)	2.279(2)	2.206(2)
Ni(1)–S(1)	2.4682(7)	2.435(1)	2.4692(5)	2.5020(5)
Ni(1)–S(2)	2.4844(9)	2.4846(9)	2.4878(5)	2.4493(5)
Ni(2)–N(8)	2.036(2)	2.168(3)	2.091(2)	2.005(2)
Ni(2)–N(4)	2.319(2)	2.410(3)	2.247(2)	2.211(2)
Ni(2)–N(5)	2.167(2)	2.128(3)	2.236(2)	2.142(2)
Ni(2)–N(6)	2.293(2)	2.202(3)	2.300(2)	2.435(2)
Ni(2)–S(1)	2.4958(8)	2.4533(9)	2.3983(5)	2.5307(5)
Ni(2)–S(2)	2.4754(7)	2.434(1)	2.4967(5)	2.4553(5)
Ni–N	2.208(2)	2.224(3)	2.210(2)	2.205(2)
Ni–S	2.4810(7)	2.452(1)	2.4630(5)	2.4843(5)
Ni···Ni	3.373(1)	3.401(1)	3.349(1)	3.373(1)
Ni–Ni^{cent}/Ni–Ni^{cent}[a]	–	–	14.040(1)	9.184(1)
N–M–N_{cis}[b]	90.73(8)	90.5(1)	90.69(6)	90.33(6)
N–M–N_{trans}[b]	176.63(7)	176.2(1)	177.04(6)	175.70(6)
S–M–N_{cis}[b]	90.83(7)	91.22(8)	91.06(5)	91.13(2)
S–M–N_{trans}[b]	170.27(6)	171.03(8)	170.22(5)	171.43(5)
S–M–S[b]	81.62(3)	81.28(3)	80.46(2)	82.10(2)
M–S–M[b]	85.65(2)	87.83(3)	85.68(2)	85.53(2)

[a] Distance between center of the Ni···Ni axes of the Ni_2 units. [b] Average values.

does the charged pyrazolato ligand in **6**. A similar behaviour has been noted previously for $[L^1Ni_2(\mathit{pydz})]^{2+}$ and $[L^1Ni_2(\mathit{pz})]$.[18] As in **6**, the coordination of the pyridazine ring to the Ni^{II} ions results in a slight elongation of the N–N bond length [N(7)–N(8) = 1.336(2) Å vs. N(9)–N(10) 1.366(2) Å]. Likewise, the two six-membered rings are also tilted by 25.2° with respect to each other. The Ni···Ni distance is at 3.401(1) Å.

Complex **8**$[BPh_4]_2\cdot 6MeCN\cdot 2H_2O$ crystallizes in the triclinic space group $P\bar{1}$ with six cocrystallized acetonitrile and two water molecules. The $[(L^1Ni_2)_2(\mathit{bpzb})]^{2+}$ complex is centrosymmetric (Figure 3). Selected bond lengths and angles are summarized in Table 1. The structure of **8** unambiguously confirms the ability of the deprotonated 1,4-bis(4′-pyrazolyl)-benzene to link two $[L^1Ni^{II}_2]^{2+}$ units. The four six-coordinate Ni atoms are arranged in a rectangular fashion, the Ni···Ni distances being 3.349(1) Å [Ni(1)···Ni(2)] and 14.040(1) Å [Ni(1)···Ni(2′)], respectively. Note that the Ni_2pyrazolato planes are coplanar with each other, but that the central aromatic ring is slightly twisted out of this plane (τ = 23.8°). The metal–ligand bond lengths within the $[L^1Ni_2(\text{pyrazolato})]^{2+}$ units reveal no anomalities and are very similar to those in **6** [Table 1]. There are no significant intermolecular interactions between the Ni_4 complexes. The shortest intermolecular Ni···Ni distance is at 7.806[1] Å.

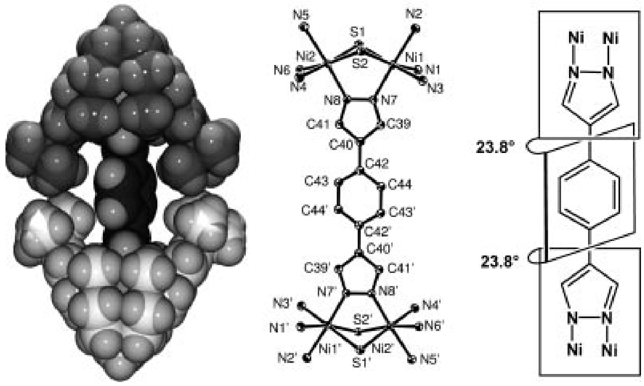

Figure 3. Left: Van der Waals plot of the $[(L^1Ni^{II}_2)_2(\mathit{bpzb})]^{2+}$ dication in crystals of **8**$[BPh_4]_2\cdot 6MeCN\cdot 2H_2O$. Middle: ORTEP representation of the core structure of **8** with the atom labeling Scheme. Ellipsoids are represented at the 50% probability level. Symmetry code used to generate equivalent atoms: 1 – *x*, 1 – *y*, 1 – *z* (′). Right: Mutual orientation of the Ni_2pyrazolato planes in **8**.

Crystals of **9**$[BPh_4]_2\cdot 2CH_2Cl_2$ are triclinic, space group $P\bar{1}$. Ortep views of the structure of the dication **9** and the central core are provided in Figure 4. A selection of the most important bond lengths is given in Table 1. Again, **9** exhibits crystallographically imposed inversion symmetry. In striking contrast to **6**, the bipyrazolate moiety in **9** behaves as a tetradentate bridging ligand joining two binuclear $[L^2Ni_2]$ subunits, most likely as a consequence of the absence of the *tert*-butyl groups in $(L^2)^{2-}$. The bipyrazolate ligand assumes a planar conformation and the Ni_2N_2 planes are only slightly folded with respect to the bipyrazolato plane (folding angle: 165.4°). The Ni···Ni distance of 3.448(1) Å is the same as that in **6**. The distance *d* between the center of the Ni···Ni axes of the binuclear subunits amounts to 9.184(1) Å, which is significantly smaller than the corresponding distance in **8**. The bond lengths and angles around the Ni atoms within the $[L^2Ni_2]^{2+}$ unit reveal no unusual features. The average Ni–S, $Ni–N_{amine}$ and $Ni–N_{pyrazolato}$ distances are at 2.018(3), 2.291(3), and 2.517(1) Å, respectively. Virtually the same distances are seen in **6**. A large number of polymeric metal complexes containing bipyrazolato ligands have been structurally characterized;[2–7] to the best of our knowledge, **9** is the first discrete species of $(\mathit{bpz})^{2-}$. Overall, this structure clearly shows that two bioctahedral $[L^2Ni_2]^{2+}$ units can be linked by bipyrazolate dianions.

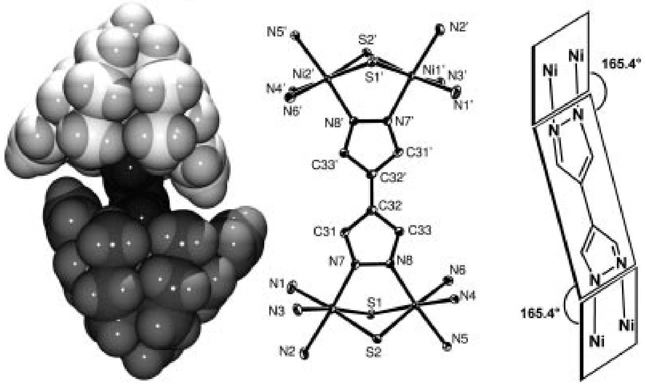

Figure 4. Left: van der Waals plot of the $[(L^2Ni^{II}_2)_2(\mu\text{-bipyrazolato})]^{2+}$ dication in crystals of **9**$[BPh_4]_2\cdot 2CH_2Cl_2$. Middle: ORTEP representation of the core structure of **9** with the atom labeling Scheme. Ellipsoids are represented at the 50% probability level. Symmetry code used to generate equivalent atoms: 1 – *x*, 2 – *y*, – *z* (′). Right: Tilting of the Ni_2pyrazolato planes in **9**.

Magnetic Properties of 9[BPh$_4$]$_2$

To gain insight into the electronic structure of **9**$[BPh_4]_2$ variable-temperature magnetic susceptibility data were measured between 2.0 and 295 K by using a SQUID magnetometer in an applied external magnetic field of 0.2 T. Figure 5 shows a plot of the temperature dependence of the effective magnetic moment for **9**$[BPh_4]_2$. The effective magnetic moment increases from 6.75 μ_B at 295 K to a maximum value of 7.59 μ_B at 22 K. On lowering the temperature further the magnetic moment decreases to 6.97 μ_B at 2.0 K. Although the effective magnetic moment at 22 K is smaller than expected for the spin-only value of 9.84 μ_B for $S_T = 4$ resulting from the ferromagnetic coupling of four Ni^{II} ions ($S_i = 1$, $g = 2.20$), it is larger than the value of 6.22 μ_B calculated for four noninteracting Ni^{II} ions. This behaviour indicates the presence of weak ferromagnetic exchange interactions between the Ni^{II} ions in the binuclear subunits but negligible – if any – coupling across the bipyrazolate bridge. This is not surprising, considering the long distance between the nickel(II) ions.

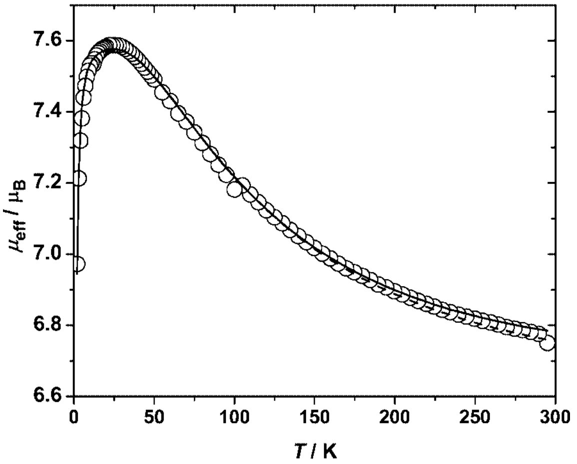

Figure 5. Temperature dependence of μ_{eff} (per tetranuclear complex) for **9**$[BPh_4]_2$. The full line represents the best theoretical fit to Equation (1). The dashed line represents the best fit to the dimer model in Equation (3).

The magnetic susceptibility data were fitted to Equation (1), where χ_{tetra} and χ_{mono} refer to the molar susceptibilities of a Ni_4 complex and a fraction ρ of a mononuclear nickel(II) impurity with Curie constant $C = Ng^2\mu_B{}^2/3kT$.

$$\chi = \chi_{tetra}(1 - \rho) + 4\chi_{mono}\rho \tag{1}$$

The molar magnetic susceptibility χ_{tetra} was derived from the appropriate spin-Hamiltonian Equation (2) including the isotropic HDVV exchange, the single-ion zero-field splitting and the single-ion Zeeman interaction by a full-matrix diagonalization approach.

$$H = -2J_1(\hat{S}_1 \cdot \hat{S}_2 + \hat{S}_3 \cdot \hat{S}_4) - 2J_2(\hat{S}_1 \cdot \hat{S}_3 + \hat{S}_1 \cdot \hat{S}_4 + \hat{S}_2 \cdot \hat{S}_3 + \hat{S}_2 \cdot \hat{S}_4)$$
$$+ \sum_{i=1}[D_i(\hat{S}_{iz}^2 - {}^1\!/_3 S_i(S_i + 1)) + g_i\mu_B S_{i\tau}B_\tau] \; (\tau = x, y, z) \tag{2}$$

In this model J_1 represents the exchange interaction between the Ni^{2+} ions within the dinuclear subunit, whereas J_2 describes the interaction across the bipyrazolate moiety. The D and g values were considered to be identical for all of the four Ni^{2+} ions. Notice that D represents an effective zero-field splitting parameter, since in Equation (2) and Equation (4) the zero-field splitting tensors of all ions are assumed to be collinear. The least-squares fitting of the experimental data over the full temperature range led to J_1 = +24.0(1) cm^{-1}, J_2 = –0.001(5) cm^{-1}, g = 2.19(1), D = 4.8(2) cm^{-1}, and ρ = 0.02(1)%. The inclusion of the D parameter improves the low-temperature fit significantly, but it represents by no means an accurate value since temperature-dependent magnetic susceptibility measurements are not very appropriate for the determination of the sign and magnitude of D.[33,34] However, this analysis establishes clearly that magnetic exchange interactions via the dipyrazolate moiety are not significant ($J_2 < 0.1$ cm^{-1}) and that the magnetic properties of complex **9** are solely based on the exchange couplings in the binuclear $[L^2Ni_2(\text{pyrazolate})]^+$ subunits. Therefore, we also tried to simulate the temperature dependence of the magnetic data by using an isotropic dimer model [Equation (3)] for two Ni^{II} (S = 1) ions based on the Hamiltonian in [Equation (4)].

$$\chi = 2[\chi_{dim}(1 - \rho) + 2\chi_{mono}\rho] \tag{3}$$

$$H = -2JS_1S_2 + \sum_{i=1}^{2}(D_i(\hat{S}_{zi}^2 - 1/3(S_i(S_i + 1)) + g_i\mu_B S_{i\tau}B_\tau)) \;\; (\tau = x, y, z) \tag{4}$$

The magnetic data could be reproduced equally well by this approach (Figure 5), yielding J_1 = +24.14 cm^{-1}, g = 2.19, D = 4.85 cm^{-1}, and ρ = 0.020%. Again, this analysis reveals a weak ferromagnetic coupling between the two Ni^{II} ions. All of these values are in excellent agreement with those reported for other dinuclear nickel(II) complexes of $(L^1)^{2-}$ providing further support for the absence of significant interdimer exchange coupling in **9**$[BPh_4]_2$.[18,24]

It should be noted that there is much interest in the distance-dependence of superexchange interactions between paramagnetic transition metal ions bridged by extended organic spacer ligands. Thus, a large number of dicarboxylato-bridged copper(II) dimers with Cu···Cu separations of 5 to 15 Å have been prepared and their magnetic properties have been determined.[35–41] The magnetic exchange interactions decrease rapidly with increasing Cu···Cu separations and the experimentally determined J values approach the values predicted by the Coffman–Buettner relation [$|J| \leq 1$ cm^{-1} for $d(M\cdots M) \geq 9$ Å].[42] This finding also applies to other paramagnetic metal ions than Cu.[43] The observations made for the nickel(II) complexes presented herein are in good agreement with the reported trend. It is also worth mentioning that the coplanarity of the two Ni_2pyrazolato planes in **9** does not strengthen the magnetic exchange interactions via the bipyrazolate moiety.

Conclusions

In summary, we presented the synthesis of two new heterocyclic N_4-ligands and the first members of a new class of tetranuclear nickel(II) complexes in which pairs of dinuclear LNi_2 fragments are united by $(bpz)^{2-}$ and $(bpzb)^{2-}$ groups. The isolation of the two dinuclear complexes **6** and **7** clearly show that the ease of formation of a tetranuclear cluster depends critically on two factors: (*i*) the length of the bridging coligand and (*ii*) the steric demand of the supporting ligand. If one pays attention to these two factors one can readily prepare higher nuclearity clusters such as **8** and **9**. These exist as stable and discrete complexes in solution and in the solid state as ascertained by various spectroscopic methods and X-ray crystallography. The Ni_4 complexes are well separated from each other in the solid state. The magnitude of the exchange interaction J_2 across the bipyrazolate was found to be less than 0.1 cm^{-1}, suggesting that no interdimer exchange coupling occurs in **9**. In this sense the LNi_2^{2+} fragments are ideally suited to screen novel extended bridging ligands for their ability to transmit magnetic exchange interactions between paramagnetic transitions metal ions.

Experimental Section

General Remarks: Solvents and reagents were of reagent grade quality and used as received unless otherwise specified. The compounds 4,4′-bipyrazol,[2] $[L^1Ni^{II}_2Cl][ClO_4]$,[15] $[L^1Ni^{II}_2(ClO_4)][ClO_4]$,[20] and $[L^2Ni^{II}_2(Cl)][ClO_4]$[16] were prepared according to the literature procedures. Melting points were determined in capillaries and are uncorrected. IR spectra were measured on a Bruker VECTOR 22 FT-IR spectrophotometer as KBr pellets, electronic absorption spectra on a Jasco V-570 UV/Vis/near IR spectrophotometer. Elemental analysis were performed on a Vario EL analyzer (Elementaranalysensysteme GmbH). All metal complexes crystallize with solvent molecules (see crystal structures), but slowly lose their solvent molecules of crystallization upon standing in air. This is why the observed microanalytical data do not fit exactly with the calculated values (for the solvent-free compounds). Temperature-dependent magnetic susceptibility measurements on powdered solid samples were carried out on a SQUID magnetometer (MPMS Quantum Design) over the temperature range 2.0 –293 K. The magnetic field applied was 0.20 Tesla. The observed susceptibility data were corrected for underlying diamagnetism by using Pascal's constants.

Safety Note: Caution! *Perchlorate salts of transition metal complexes are potentially hazardous and may explode. Only small quantities should be prepared and handled with great care.*

4,4′-Bipyridazine (*bpdz*): A solution of 12.31 g (0.15 mol) 1,2,4,5-tetrazine (**1**) in 150 mL of dry 1,4-dioxane was added dropwise for a period of 40 min to a stirred solution of 10.09 g (0.072 mol) of *cis-trans*-1,4-bis(dimethylamino)butadiene (**2**) in 60 mL of dry 1,4-dioxane. The immediate evolution of nitrogen gas and discoloration were accompanied with a pronounced exothermic effect. After the addition was completed, the red-brown reaction mixture was stirred at 80 °C for 4 h (elimination of dimethylamine) and then left overnight at room temp. The precipitate was filtered, washed with 5 mL CH_2Cl_2 and twice crystallized from methanol with charcoal yielding a pure product (4.44 g, 39%) as thin colorless needles. ^1H NMR (400 MHz, $[D_6]$DMSO): $\delta = 9.77$ (s, 2 H, 3-CH), 9.37 (d, 2 H, 6-CH), 8.23 (dd, 2 H, 5-CH) ppm. $C_8H_6N_4$ (158.16): calcd. C 60.75, H 3.82, N 35.43; found C 60.44, H 3.89, N 35.17.

1,4-Bis(4′-pyrazolyl)benzene. Intermediate 4: 11.2 mL (0.12 mol) $POCl_3$ was added dropwise to 45 mL of dry DMF at 5–10 °C with constant stirring. The mixture was stirred for an additional hour at room temp. Then 3.88 g (20.0 mmol) solid *p*-phenylenediacetic acid (**3**) was added at once and the clear solution formed was stirred for 4 h at 90–95 °C and then at room temperature overnight. The resulting black mixture was poured on 100 g crushed ice. After decomposition of the excess Vilsmeyer reagent a saturated solution of 15.0 g $NaClO_4$ was added with stirring. The resulting nearly white crystalline deposit of the bis(trimethinium) diperchlorate (**4**$[ClO_4]_2$) was filtered and washed with two 15 mL portions of water. The yield was 8.21 g (79.5%). This compound was used in the next step without further purification. **Intermediate 5:** 8.22 g (15.6 mmol) of the perchlorate salt **4**$[ClO_4]_2$ were added to a warm solution of 3.45 g (86 mmol) NaOH in 20 mL water, and the mixture was heated with stirring for 7–8 min (bath temperature 90 °C) until total dissolution of the organic salt was observed. The yellow-colored mixture was cooled to room temp., diluted with 10 mL water and 10% HCl solution was added to pH = 5, leading to precipitation of the tetraaldehyde **5**. Then 5.0 mL hydrazine hydrate was added at once with stirring, which effects dissolution of **5** and after 15–20 min stirring at room temp. the dipyrazole H_2*bpzb* deposits as thin white needles. The mixture was left overnight and filtered to yield 3.22 g (98.5%) of the product. This compound was used for the preparation of the metal complexes without further purification.

$[L^1Ni_2(H$*bpz*$)][ClO_4]$ (6$[ClO_4]$): To a solution of H_2*bpz* (13.8 mg, 0.103 mmol) in methanol (30 mL) was added triethylamine (20 mg, 0.20 mmol). Complex $[L^1Ni_2Cl][ClO_4]$ (194 mg, 0.210 mmol) was added and the resulting yellow solution was stirred for 12 h. A solution of $LiClO_4·3H_2O$ (160 mg, 1.00 mmol) in methanol (2 mL) was then added. After further stirring for 12 h, the green precipitate was filtered, washed with cold ethanol, and dried in air. Yield: 80 mg (76%). M.p. 363–365 °C (decomp.). IR (KBr): $\tilde{\nu} = 3394$ (m), 2961 (s), 2867 (s), 1629 (w), 1463 (s), 1394 (w), 1363 (w), 1311 (w), 1265 (w), 1236 (w), 1203 (w), 1151 (m), 1078 [vs, $\nu_3(ClO_4^-)$], 1057 (s), 1041 (s), 1008 (w), 914 (m), 882 (w), 825 (m), 754 (w), 657 (w), 626 [m, $\nu_4(ClO_4^-)$], 563 (w), 535 (w), 492 (w), 461 (w), 418 (w). UV/Vis (CH_3CN): λ_{max}/nm (ε/$M^{-1}\,cm^{-1}$) = 385 (1064), 634 (13), 1187 (24).

$[L^1Ni_2(H$*bpz*$)][BPh_4]$ (6$[BPh_4]$): To a solution of **6**$[ClO_4]$ (102 mg, 0.100 mmol) in methanol (50 mL) was added a solution of $NaBPh_4$ (342 mg, 1.00 mmol) in methanol (50 mL). The reaction mixture was allowed to stir for 3 h. The green product was filtered, washed with ethanol, and dried in air to give 113 mg (91%) of **6**$[BPh_4]$ as a green, air-stable, microcrystalline powder. M.p. 295–297 °C (decomp.). IR (KBr): $\tilde{\nu} = 3384$ (m), 3123 (w), 3054 (m), 3032 (m), 2963 (s), 2858 (s), 1944 (w), 1877 (w), 1815 (w), 1764 (w), 1622 (w), 1580 (w), 1524 (w), 1462 (s), 1425 (m), 1393 (m), 1363 (m), 1309 (w), 1265 (m), 1235 (m), 1201 (w), 1169 (w), 1151 (w), 1126 (w), 1075 (m), 1040 (s), 1006 (w), 928 (w), 912 (m), 881 (w), 824 (m), 733 [s, $\nu(BPh_4^-)$], 704 [s, $\nu(BPh_4^-)$], 628 (m), 611 (m), 562 (w), 534 (w), 492 (w), 467 (w), 430 (w), 417 (w). UV/Vis (CH_3CN): λ_{max}/nm (ε/$M^{-1}\,cm^{-1}$) = 382 (1037), 634 (14), 1182 (24). $C_{68}H_{89}BN_{10}Ni_2S_2$ (1238.83): calcd. C 65.93, H 7.24, N 11.31, S 5.18; found C 65.50, H 7.53, N 11.00, S 4.96. Single crystals of **6**$[BPh_4]·1.5MeCN$ suitable for X-ray structure analysis were grown by slow evaporation of an ethanol/acetonitrile solution of **6**$[BPh_4]$. These crystals slowly lose the solvent molecules of solvent of crystallization at ambient temperature and become turbid.

$[L^1Ni_2($*bpdz*$)][ClO_4]_2$ (7$[ClO_4]_2$): To a solution of $[L^1Ni_2Cl][ClO_4]$ (92 mg, 0.10 mmol) in methanol (30 mL) was added solid $Pb(ClO_4)_2$ (80 mg, 0.20 mmol). The color of the reaction mixture immediately turned from yellow to dark green. The reaction mixture was stirred for 5 min, filtered off from $PbCl_2$, and to the dark-green filtrate was added a solution of *bpdz* (7.9 mg, 0.050 mmol) in acetonitrile (5 mL) to give a brown-yellow solution. The solution was kept at room temperature for three days during which time brown crystals separated. These were isolated by filtration, washed with a little amount of cold methanol, and dried in air. Yield: 91 mg (80%). M.p. 297–298 °C (decomp.). IR (KBr): $\tilde{\nu} = 3433$ (m), 2962 (s), 2868 (s), 2250 (w), 2017 (w), 1603 (w), 1581 (m), 1464 (s), 1395 (m), 1364 (m), 1310 (m), 1267 (m), 1235 (m), 1199 (w), 1094 [vs, $\nu_3(ClO_4^-)$], 912 (m), 887 (m), 850 (w), 824 (s), 755 (w), 688 (w), 669 (w), 624 [s, $\nu_4(ClO_4^-)$], 566 (w), 538 (w), 494 (w), 440 (w), 414 (w) cm^{-1}. UV/Vis (CH_3CN): λ_{max}/nm (ε/$M^{-1}\,cm^{-1}$) = 608 (47), 1094 (51). $C_{46}H_{70}Cl_2N_{10}Ni_2O_8S_2$ (1143.53): calcd. C 48.31, H 6.17, N 12.25, S 5.61; found C 48.25, H 5.98, N 11.95, S 5.32. The crystals of **7**$[ClO_4]_2·3MeCN$ used for an X-ray structure determination were picked from the mother liquor.

$[(L^1Ni_2)_2(\mathit{bpzb})][ClO_4]_2$ (8$[ClO_4]_2$): To a solution of $H_2\mathit{bpzb}$ (21 mg, 0.10 mmol) in methanol (50 mL) and triethylamine (20 mg, 0.20 mmol) was added solid $[L^1Ni_2Cl][ClO_4]$ (184 mg, 0.200 mmol). The mixture was stirred for 3 d during which time the colour of the suspension changed from yellow to green. A solution of $LiClO_4{\cdot}3H_2O$ (320 mg, 2.00 mmol) in methanol (10 mL) was added. After stirring for 1 d, the green precipitate was collected by filtration, washed several times with cold ethanol and dried in air. Yield: 150 mg (76%). M.p. 342–343 °C (decomp.). IR (KBr): $\tilde{\nu}$ = 3431 (s), 2962 (s), 2866 (s), 1630 (w), 1579 (w), 1462 (s), 1395 (w), 1363 (w), 1310 (w), 1266 (w), 1233 (m), 1201 (w), 1150 (m), 1121 (s), 1077 [vs, $\nu(ClO_4^-)$], 1057 (s), 1041 (s), 1000 (w), 956 (w), 928 (w), 913 (w), 881 (w), 826 (m), 807 (w), 754 (w), 625 [m, $\nu_4(ClO_4^-)$], 564 (w), 535 (w), 493 (w), 413 (w) cm^{-1}. UV/Vis (CH_3CN): λ_{max}/nm (ε/$M^{-1}\,cm^{-1}$) = 380 (4989), 627 (57), 1195 (132).

$[(L^1Ni_2)_2(\mathit{bpzb})][BPh_4]_2$ (8$[BPh_4]_2$): To a solution of 8$[ClO_4]_2$ (198 mg, 0.100 mmol) in methanol (50 mL) was added a solution of $NaBPh_4$ (684 mg, 2.00 mmol) in methanol (10 mL). The reaction mixture was allowed to stir for 1 h, and the volume of the solution reduced in vacuo to about 30 mL. The green product was filtered, washed with ethanol and dried in air to give 189 mg (78%) of 8$[BPh_4]_2$ as a green, air-stable, microcrystalline powder. M.p. 350–351 °C (decomp.). IR (KBr): $\tilde{\nu}$ = 3435 (s), 3054 (m), 3027 (m), 2963 (s), 2866 (s), 1636 (w), 1579 (w), 1480 (m), 1462 (s), 1395 (w), 1363 (w), 1310 (w), 1266 (w), 1233 (m), 1201 (w), 1169 (w), 1152 (w), 1122 (w), 1108 (w), 1076 (m), 1056 (m), 1042 (s), 1000 (w), 956 (w), 928 (w), 912 (w), 881 (w), 825 (s), 733 [s, $\nu(BPh_4^-)$], 704 [s, $\nu(BPh_4^-)$], 629 (w), 612 (m), 564 (w), 535 (w), 492 (w), 445 (w) cm^{-1}. UV/Vis (CH_3CN): λ_{max}/nm (ε/$M^{-1}\,cm^{-1}$) = 381 (4626), 631 (53), 1190 (112). $C_{136}H_{176}B_2N_{16}Ni_4S_4$ (2419.62): calcd. C 67.51, H 7.33, N 9.26, S 5.30; found C 66.92, H 7.39, N 9.15, S 4.82. Single crystals of 8$[BPh_4]{\cdot}6MeCN{\cdot}2H_2O$ suitable for X-ray structure analysis were grown by slow evaporation of an ethanol/acetonitrile solution of 8$[BPh_4]$.

$[(L^2Ni_2)_2(\mathit{bpz})][ClO_4]_2$ (9$[ClO_4]_2$): To a solution of $H_2\mathit{bpz}$ (13.4 mg, 0.100 mmol) in methanol (30 mL) was added triethylamine (20 mg, 0.20 mmol). Complex $[L^2Ni_2Cl][ClO_4]$ (162 mg, 0.200 mmol) was slowly added resulting in the immediate formation of a green precipitate. After the addition was complete, further $LiClO_4{\cdot}3H_2O$ (320 mg, 2.00 mmol) dissolved in methanol (2 mL) was added, and stirring was continued for additional 12 h. The green product was collected by filtration, washed several times with cold methanol, and dried in air. Yield: 123 mg (73%). M.p. 340–341 °C (decomp.). IR (KBr): $\tilde{\nu}$ = 3521 (m), 2969 (s), 2855 (s), 2245 (w), 2017 (w), 1628 (w), 1587 (m), 1487 (s), 1454 (s), 1435 (s), 1396 (m), 1364 (w), 1350 (w), 1298 (m), 1268 (s), 1254 (m), 1200 (w), 1170 (m), 1095 [vs, $\nu_3(ClO_4^-)$], 1042 (s), 999 (m), 956 (w), 916 (s), 897 (w), 828 (s), 806 (m), 764 (s), 727 (w), 670 (m), 655 (w), 623 [s, $\nu_4(ClO_4^-)$], 566 (w), 537 (w), 489 (w), 462 (w), 433 (w), 412 (w) cm^{-1}. UV/Vis (CH_3CN): λ_{max}/nm (ε/$M^{-1}\,cm^{-1}$) = 294 (23213), 380 (3785), 635 (66), 1178 (91).

$[(L^2Ni_2)_2(\mathit{bpz})][BPh_4]_2$ (9$[BPh_4]_2$): To a warm solution of 9$[ClO_4]_2$ (168 mg, 0.100 mmol) in methanol (50 mL) was added a solution of $NaBPh_4$ (342 mg, 1.00 mmol) in methanol (100 mL). The reaction mixture was allowed to stir for 3 h. The green microcrystalline precipitate was filtered, washed with ethanol and dried in air yielding 186 mg (88%) of 9$[BPh_4]_2$ as a green powder. M.p. 335–336 °C (decomp.). IR (KBr): $\tilde{\nu}$ = 3523 (w), 3054 (m), 2984 (s), 2854 (s), 2247 (w), 1634 (w), 1586 (m), 1484 (m), 1463 (s), 1435 (s), 1396 (m), 1364 (m), 1350 (w), 1337 (w), 1297 (m), 1267 (s), 1255 (m), 1200 (w), 1169 (m), 1095 (s), 1075 (s), 1041 (s), 998 (m), 956 (m), 916 (s), 896 (m), 827 (s), 806 (m), 761 (s), 732 [s, $\nu(BPh_4^-)$], 704 [s, $\nu(BPh_4^-)$], 669 (m), 623 (s), 612 (m), 565 (w), 536 (w), 488 (w), 465 (w), 433 (w), 412 (w) cm^{-1}. UV/Vis (CH_3CN): λ_{max}/nm (ε/$M^{-1}\,cm^{-1}$) = 294 (27244), 376 (4504), 637 (63), 1183 (111). $C_{114}H_{140}B_2N_{16}Ni_4S_4$ (2119.09): calcd. C 64.61, H 6.66, N 10.58, S 6.05; found C 62.79, H 6.81, N 11.43, S 5.92. Single crystals of 9$[BPh_4]_2{\cdot}2CH_2Cl_2$ suitable for X-ray structure analysis were grown by recrystallization from dichloromethane.

Collection and Reduction of X-ray Data: Suitable single crystals of 6$[BPh_4]{\cdot}1.5MeCN$, 7$[ClO_4]_2{\cdot}3MeCN$, 8$[BPh_4]_2{\cdot}6MeCN{\cdot}2H_2O$, and 9$[BPh_4]_2{\cdot}2CH_2Cl_2$ were selected and mounted on the tip of a glass fibre using perfluoropolyether oil. The data sets were collected at 213(2) K using a STOE IPDS-2T diffractometer. Graphite-mono-

Table 2. Crystallographic data for complexes 6$[BPh_4]{\cdot}1.5MeCN$, 7$[ClO_4]_2{\cdot}3MeCN$, 8$[BPh_4]_2{\cdot}6MeCN{\cdot}2H_2O$, and 9$[BPh_4]_2{\cdot}2CH_2Cl_2$.

Compound	6$[BPh_4]{\cdot}1.5MeCN$	7$[ClO_4]_2{\cdot}3MeCN$	8$[BPh_4]_2{\cdot}6MeCN{\cdot}2H_2O$	9$[BPh_4]_2{\cdot}2CH_2Cl_2$
Formula	$C_{71}H_{93.50}BN_{11.50}Ni_2S_2$	$C_{52}H_{79}Cl_2N_{13}Ni_2O_8S_2$	$C_{148}H_{198}B_2N_{22}Ni_4O_2S_4$	$C_{116}H_{144}B_2Cl_4N_{16}Ni_4S_4$
M_r [g/mol]	1300.42	1266.72	2701.98	2288.97
Space group	$P\bar{1}$	$P\bar{1}$	$P\bar{1}$	$P\bar{1}$
a [Å]	12.5151(13)	13.2202(9)	13.9142(4)	12.2969(5)
b [Å]	16.2376(14)	15.6825(10)	16.0978(5)	15.3907(6)
c [Å]	18.270(2)	16.7954(10)	18.6102(6)	15.5812(7)
α [°]	98.745(12)	74.250(8)	108.658(2)	73.445(3)
β [°]	95.316(12)	69.252(8)	107.475(2)	80.928(3)
γ [°]	103.121(11)	66.228(8)	102.448(3)	79.567(3)
V [Å^3]	3542.4(6)	2946.2(3)	3536.1(2)	2762.2(2)
Z	2	2	1	1
$d_{calcd.}$ g/cm^3	1.219	1.428	1.269	1.376
Cryst. size [mm]	0.30 × 0.25 × 0.25	0.27 × 0.24 × 0.18	0.30 × 0.30 × 0.15	0.30 × 0.20 × 0.15
μ(Mo-K_α) [mm^{-1}]	0.639	0.864	0.643	0.900
θ limits [°]	2.37–28.04	5.84–25.98	3.31–33.29	3.36–28.00
Measured reflections	24520	23694	59533	19250
Independent reflections	15783	10610	23987	13319
Observed reflections[a]	10159	5881	18472	11233
Number of parameters	778	727	845	659
R_1[b] (R_1 all data)	0.0399 (0.0571)	0.0417 (0.0826)	0.0526 (0.0713)	0.0370 (0.0443)
wR_2[c] (wR_2 all data)	0.1111 (0.1142)	0.0874 (0.0932)	0.1383 (0.1478)	0.1092 (0.1121)
Max., min. peaks, [e/Å^3]	0.994, –0.751	0.602, –0.570	1.105, –1.256	1.349, –1.563

[a] Observation criterion: $I > 2\sigma(I)$. [b] $R_1 = \Sigma\|F_o| - |F_c\|/\Sigma|F_o|$. [c] $wR_2 = \{\Sigma[w(F_o^2 - F_c^2)^2]/\Sigma[w(F_o^2)^2]\}^{1/2}$.

chromated Mo-K_α radiation (λ = 0.71073 Å) was used throughout. The data were processed with the program STOE X-AREA.[44] Selected details of the data collection and refinement are given in Table 2. The structures were solved by direct methods[45] and refined by full-matrix least-squares techniques on the basis of all data against F^2 using SHELXL-97.[46] PLATON was used to search for higher symmetry.[47] All non-hydrogen atoms were refined anisotropically. H atoms were placed at calculated positions and refined as riding atoms with isotropic displacement parameters.

Some of the solvate molecules in **6** and **7** were found to be disordered or only partially occupied. In the crystal structure of **6**[BPh$_4$]$_2$·1.5MeCN the occupancy factor of one MeCN was reduced to 0.5. In the crystal structure of **7**[BPh$_4$]$_2$·6MeCN·2H$_2$O the water molecule was found to be disordered over two sites. The respective orientations were refined by using a split atom model to give site occupancy factors of 0.59(1) [O(1a)] and 0.41(1) [for O(1b)]. Water hydrogen atoms were not included in the refinement. Graphics were produced with Ortep3 for Windows.[48]

CCDC-641207 (for **2**), -641208 (for **3**), -641209 (for **4**), and -641210 (for **5**) contain the supplementary crystallographic data for this paper. These data can be obtained free of charge from the Cambridge Crystallographic Data Centre via www.ccdc.cam.ac.uk/data_request/cif.

Supporting Information (see also the footnote on the first page of this article): Experimental and calculated magnetic values susceptibility data for **9**[BPh$_4$]$_2$.

Acknowledgments

We sincerely thank the Deutsche Forschungsgemeinschaft (DFG) (priority program 1137 “Molecular Magnetism”) for funding of this work. We are grateful to Prof. Dr. F. Meyer for providing facilities for magnetic susceptibility measurements.

---

[1] S. Trofimenko, *J. Org. Chem.* **1964**, *29*, 3046–3049.

[2] I. Boldog, J. Sieler, A. N. Chernega, K. V. Domasevitch, *Inorg. Chim. Acta* **2002**, *338*, 69–77.

[3] P. E. Kruger, G. D. Fallon, B. Moubaraki, K. S. Murray, *J. Chem. Soc., Chem. Commun.* **1992**, 1926–1927.

[4] a) V. V. Ponomarova, V. V. Komarchuk, I. Boldog, A. N. Chernega, J. Sieler, K. Domasevitch, *Chem. Commun.* **2002**, 436–437; b) I. Boldog, E. B. Rusanov, J. Sieler, S. Blaurock, K. V. Domasevitch, *Chem. Commun.* **2003**, 740–741; c) E. B. Rusanov, V. V. Ponomarova, V. V. Komarchuk, H. Stoeckli-Evans, E. Fernandez-Ibanez, F. Stoeckli, J. Sieler, K. V. Domasevitch, *Angew. Chem.* **2003**, *115*, 2603–2605; *Angew. Chem. Int. Ed.* **2003**, *42*, 2499–2501.

[5] J.-P. Zang, S. Horike, S. Kitagawa, *Angew. Chem.* **2007**, *119*, 907–910; *Angew. Chem. Int. Ed.* **2007**, *46*, 889–892.

[6] J. He, Y.-G. Yin, T. Wu, D. Li, X.-C. Huang, *Chem. Commun.* **2006**, 2845–2847.

[7] a) M. Eddaoudi, D. B. Moler, H. Li, B. Chen, T. M. Reineke, M. O'Keeffe, O. M. Yaghi, *Acc. Chem. Res.* **2001**, *34*, 319–330; b) M. Eddaoudi, J. Kim, J. B. Wachter, H. K. Chae, M. O'Keeffe, O. M. Yaghi, *J. Am. Chem. Soc.* **2001**, *123*, 4368–4369; c) J. L. C. Rowsell, A. R. Millward, K. S. Park, O. M. Yaghi, *J. Am. Chem. Soc.* **2004**, *126*, 5666–5667; d) T. J. Barton, L. M. Bull, W. G. Klemperer, D. A. Loy, B. McEnaney, M. Misono, P. A. Monson, G. Pez, G. W. Scherer, J. C. Vartuli, O. M. Yaghi, *Chem. Mater.* **1999**, *11*, 2633–2656.

[8] C. N. R. Rao, S. Natarajan, A. Choudhury, S. Neeraj, A. A. Ayi, *Acc. Chem. Res.* **2001**, *34*, 80–87.

[9] B. Moulton, M. J. Zaworotko, *Chem. Rev.* **2001**, *101*, 1629–1658.

[10] S. Kitagawa, S. Noro, T. Nakamura, *Chem. Commun.* **2006**, 701–707.

[11] S. Kitagawa, R. Kitaura, S. Noro, *Angew. Chem.* **2004**, *116*, 2388–2430; *Angew. Chem. Int. Ed.* **2004**, *43*, 2334–2375.

[12] I. Boldog, E. B. Rusanov, A. N. Chernega, J. Sieler, K. V. Domasevitch, *Angew. Chem.* **2001**, *113*, 3543–3546; *Angew. Chem. Int. Ed.* **2001**, *40*, 3435–3438.

[13] K. V. Domasevitch, I. Boldog, *Acta Crystallogr., Sect. C* **2005**, *61*, 373–376.

[14] S. Y. Yu, H.-P. Huang, S.-H. Liu, Q. Jia, Y.-Z. Li, B. Wu, Y. Sei, K. Yamaguchi, Y.-J. Pan, H.-W. Ma, *Inorg. Chem.* **2005**, *44*, 9471–9488.

[15] B. Kersting, G. Steinfeld, *Chem. Commun.* **2001**, 1376–1377.

[16] a) G. Steinfeld, V. Lozan, B. Kersting, *Angew. Chem.* **2003**, *115*, 2363–2365; *Angew. Chem. Int. Ed.* **2003**, *42*, 2261–2263; b) S. Käss, T. Gregor, B. Kersting, *Angew. Chem.* **2006**, *118*, 107–110; *Angew. Chem. Int. Ed.* **2006**, *45*, 101–104.

[17] M. H. Klingele, G. Steinfeld, B. Kersting, *Z. Naturforsch., Teil B* **2001**, *56*, 901–907.

[18] J. Hausmann, M. H. Klingele, V. Lozan, G. Steinfeld, D. Siebert, Y. Journaux, J. J. Girerd, B. Kersting, *Chem. Eur. J.* **2004**, *10*, 1716–1728.

[19] Y. Journaux, V. Lozan, J. Hausmann, B. Kersting, *Chem. Commun.* **2006**, 83–84.

[20] V. Lozan, B. Kersting, *Eur. J. Inorg. Chem.* **2007**, 1436–1443.

[21] V. Lozan, B. Kersting, *Inorg. Chem.* **2006**, *45*, 5630–5634.

[22] B. Kersting, *Angew. Chem.* **2001**, *113*, 4110–4112; *Angew. Chem. Int. Ed.* **2001**, *40*, 3988–3990.

[23] B. Kersting, G. Steinfeld, *Inorg. Chem.* **2002**, *41*, 1140–1150.

[24] Y. Journaux, T. Glaser, G. Steinfeld, V. Lozan, B. Kersting, *Dalton Trans.* **2006**, 1738–1748.

[25] *Magnetism: Molecules to Materials* (Eds.: J. S. Miller, M. Drillon), Wiley-VCH, Weinheim, **2001**.

[26] E. Coronado, P. Delhaes, D. Gatteschi, J. S. Miller (Eds.), *Molecular magnetism: From Molecular Assmblies to Devices*, NATO ASI Series, Kluwer, Dordrecht, The Netherlands, **1995**, vol. 321.

[27] S. P. Watton, P. Fuhrmann, L. E. Pence, A. Caneschi, A. Cornia, G. L. Abbati, S. J. Lippard, *Angew. Chem.* **1997**, *109*, 2917–2919; *Angew. Chem. Int. Ed. Engl.* **1997**, *36*, 2774–2776.

[28] J. Larionova, M. Gross, M. Pilkington, H. Andres, H. Stoeckli-Evans, H. U. Güdel, S. Decurtins, *Angew. Chem.* **2000**, *112*, 1667–1672; *Angew. Chem. Int. Ed.* **2000**, *39*, 1605–1609.

[29] A. L. Dearden, S. Parsons, R. E. P. Winpenny, *Angew. Chem.* **2001**, *113*, 155–158; *Angew. Chem. Int. Ed.* **2001**, *40*, 151–154.

[30] S. Demeshko, G. Leibeling, S. Dechert, F. Meyer, *Dalton Trans.* **2006**, 3458–3465.

[31] B. Kersting, G. Steinfeld, D. Siebert, *Chem. Eur. J.* **2001**, *7*, 4253–4258.

[32] C. C. Barton, G. F. Daves, G. Franceschi, *J. Chem. Soc., Perkin Trans.* **1980**, 643–647.

[33] T. Beissel, T. Glaser, F. Kesting, K. Wieghardt, B. Nuber, *Inorg. Chem.* **1996**, *35*, 3936–3947.

[34] K. K. Nanda, A. W. Addison, N. Paterson, E. Sinn, L. K. Thompson, U. Sakaguchi, *Inorg. Chem.* **1998**, *37*, 1028–1036.

[35] T. R. Felthouse, E. J. Laskowski, D. N. Hendrickson, *Inorg. Chem.* **1977**, *16*, 1077–1089.

[36] a) M. Julve, M. Verdaguer, A. Gleizes, M. Philoche-Levisalles, O. Kahn, *Inorg. Chem.* **1984**, *23*, 3808–3818; b) S. Alvarez, M. Julve, M. Verdaguer, *Inorg. Chem.* **1990**, *29*, 4500–4507.

[37] M. Verdaguer, J. Gouteron, S. Jeannin, Y. Jeannin, O. Kahn, *Inorg. Chem.* **1984**, *23*, 4291–4296.

[38] a) E. G. Bakalbassis, C. A. Tsipis, J. Mrozinski, *Inorg. Chem.* **1985**, *24*, 4231–4233; b) E. G. Bakalbassis, J. Mrozinski, C. A. Tsipis, *Inorg. Chem.* **1986**, *25*, 3684–3690; c) C. E. Xanthopoulos, M. P. Sigalas, G. A. Katsoulos, C. A. Tsipis, A. Terzis, M. Mentzafos, A. Hountas, *Inorg. Chem.* **1993**, *32*, 5433–5436.

[39] P. Chaudhuri, K. Oder, K. Wieghardt, S. Gehring, W. Haase, B. Nuber, J. Weiss, *J. Am. Chem. Soc.* **1988**, *110*, 3657–3658.

[40] K. S. Burger, P. Chaudhuri, K. Wieghardt, B. Nuber, *Chem. Eur. J.* **1995**, *1*, 583–589.
[41] C. Erasmus, W. Haase, *Spectrochim. Acta, Ser. A* **1994**, *50*, 2189–2195.
[42] R. E. Coffman, G. R. Buettner, *J. Phys. Chem.* **1979**, *83*, 2387–2392.
[43] J. Cano, G. De Munno, J. L. Sanz, R. Ruiz, J. Faus, F. Lloret, M. Julve, A. Caneschi, *J. Chem. Soc., Dalton Trans.* **1997**, 1915–1923.
[44] *XAREA*, Stoe & Cie, Darmstadt, Germany, **2001**.
[45] G. M. Sheldrick, *Acta Crystallogr., Sect. A* **1990**, *46*, 467–473.
[46] G. M. Sheldrick, *SHELXL-97*, Computer program for crystal structure refinement, University of Göttingen, Göttingen, Germany, **1997**.
[47] Spek, A. L. *PLATON – A Multipurpose Crystallographic Tool*, Utrecht University, Utrecht, The Netherlands, **2000**.
[48] L. J. Farrugia, *J. Appl. Crystallogr.* **1997**, *30*, 565.

Received: March 22, 2007